

Edge stability, reconstruction, zero-energy states and magnetism in triangular graphene quantum dots with zigzag edges

O. Voznyy,¹ A. D. Güçlü,¹ P. Potasz,^{1,2} and P. Hawrylak¹

¹*Institute for Microstructural Sciences, National Research Council of Canada, Ottawa, Canada*

²*Institute of Physics, Wrocław University of Technology, Wrocław, Poland*

(Dated: September 17, 2018)

We present the results of ab-initio density functional theory based calculations of the stability and reconstruction of zigzag edges in triangular graphene quantum dots. We show that, while the reconstructed pentagon-heptagon zigzag edge structure is more stable in the absence of hydrogen, ideal zigzag edges are energetically favored by hydrogen passivation. Zero-energy band exists in both structures when passivated by hydrogen, however in case of pentagon-heptagon zigzag, this band is found to have stronger dispersion, leading to the loss of net magnetization.

Graphene, a single layer honeycomb lattice of carbon atoms, exhibits fascinating properties due to relativistic-like nature of quasiparticle dispersion close to the Fermi level[1–5]. Graphene’s potential for nanoelectronics applications motivated considerable amount of research in graphene nanoribbons[6–10] and, more recently, graphene quantum dots[11–24]. In such low-dimensional structures, the character of the edge drastically affects the electronic properties near the Fermi level[24–27]. In particular, assuming stable zigzag edge in triangular graphene quantum dots (TGQDs), tight-binding and density functional theory based methods predicted collapse of the energy spectrum near the Fermi level to a shell of degenerate states, isolated from the rest of the spectrum by a well defined gap[16–21, 23, 24]. It was shown that in this band of degenerate states, strong electron-electron interactions lead to ferromagnetism with peculiar magnetic[19, 21] and optical[22] properties. Recently, the potential of nanoscale graphene flakes for use in photovoltaics was demonstrated[28]. Demonstration of multiexciton generation in carbon nanotubes[29, 30] suggests its possibility in other graphene-related materials. Combined with the possibility to control the bandgap and with the presence of intermediate band in the gap, it makes TGQDs an attractive material for third generation solar cells[31].

The stability[8, 32–35], control over[10, 36, 37], and physical effects[24–27] of edges in graphene structures were studied experimentally and theoretically. It was predicted[8, 32, 34] that in nanoribbons the zigzag configuration (ZZ) is not necessarily the most stable, but a transition to reconstructed edge, terminated by pentagon-heptagon pairs (ZZ_{57}), can occur. The ZZ_{57} reconstruction was also observed experimentally[33, 34, 38] in graphene boundaries. In general, confining Dirac fermions in two-dimensions requires the understanding of the role of the edges in finite area graphene based nanostructures.

In this work, using ab-initio methods we investigate the reconstruction of the edges and corners of TGQDs and their effect on zero-energy states and magnetism. We

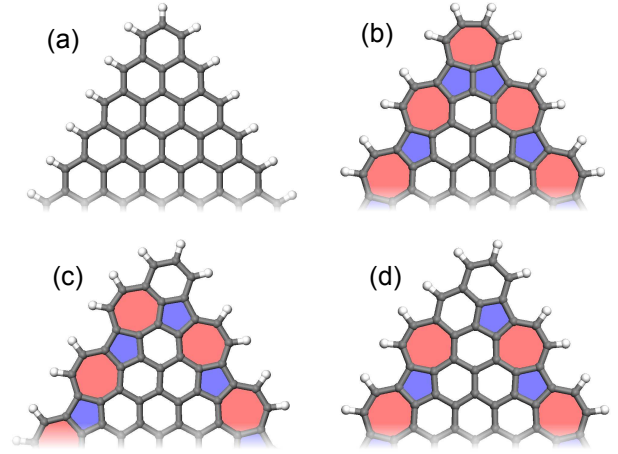


FIG. 1: (Color online) Triangular graphene quantum dot edge configurations considered in this work: (a) Ideal zigzag edges, ZZ , (b) ZZ_{57} reconstruction with pentagon-heptagon-pentagon corner configuration, (c) ZZ_{57} reconstruction with heptagon-hexagon-pentagon corner, and (d) ZZ_{57} reconstruction with hexagon-hexagon-pentagon corner.

focus on the competition between ZZ and ZZ_{57} configurations which were shown to be the most stable in previous works[8, 32, 34]. For hydrogen passivated edges, we find ZZ structure to be the most stable. We show that, in TGQDs, the reconstruction can occur in various ways due to the presence of corners, and the most stable reconstructions cause breaking of the reflection symmetry of the triangular structure. Moreover, in hydrogen passivated ZZ_{57} structures, zero energy states survive, although the ferromagnetism is destroyed due to stronger dispersion.

Calculations have been performed within the density functional theory (DFT) approach as implemented in the SIESTA code[39]. We have used the generalized gradient approximation (GGA) with the Perdew-Burke-Ernzerhof exchange-correlation functional (PBE)[40], double- ζ plus polarization orbital (DZP) bases for all atoms (i.e. $2s$, $2p$ and $2d$ orbitals for carbon, thus, both σ - and π -bonds are included on equal footing) and Troullier-Martins norm-

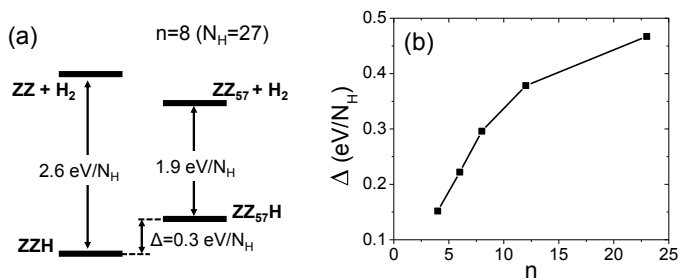


FIG. 2: (a) Relative total energies of hydrogen-passivated and non-passivated TGQDs with reconstructed and non-reconstructed edges. Presented values are per hydrogen atom for the case of $n = 8$ ($N_H = 27$) (b) Total energy difference between hydrogen-passivated ZZ_{57} and ZZ configurations as a function of number of atoms on a side of the triangle.

conserving pseudopotentials to represent the cores, 300 Ry real space mesh cutoff for charge density, and a supercell with at least 20 \AA of vacuum between the periodic images of the TGQDs. Geometries were optimized until the forces on atoms below 40 meV/\AA were reached and exactly the same geometries were used for the comparison of total energies of the ferromagnetic (FM) and antiferromagnetic (AFM) configurations. Our optimized C-C bond length for bulk graphene of 1.424 \AA overestimates the experimental value by $\sim 3\%$, typical for GGA.

Figure 1 shows different TGQD structures considered in this work. Depending on the parity of the amount of atoms in the edge of TGQD, the requirement of the ZZ_{57} reconstruction of the edge leads to several possible structures of the triangle corner, presented in Fig.1(b)-(d) (for the sake of comparison of total energies we investigate only those reconstructions conserving the amount of atoms). The three rings at the corner can have 5-7-5 (Fig.1(b)), 7-6-5 (Fig.1(c)), or 6-6-5 arrangements (Fig.1(d)). Among reconstructed corners, only the structure in Fig.1(b) conserves the mirror symmetry of the TGQD, however, according to our calculations, it is the least stable due to strong distortion of the corner cells. Thus, in the remainder of the work we will be presenting results utilizing configuration shown in Fig.1(c) for even, and that in Fig.1(d) for odd number of atoms n on a side of the triangle.

Passivation by hydrogen is an important requirement for the observation of attractive properties of TGQDs (zero-energy band of nonbonding states and magnetization of edges) which arise from topological frustration of the π -bonds [19]. Our calculations show that without hydrogen passivation, the π -bonds hybridize with the σ -bonds on the edge, destroying the zero-energy band. In Fig.2(a) we address the stability of hydrogen passivation for ZZ and ZZ_{57} edges on the example of a triangle with $n = 8$ atoms on a side (97 carbon atoms total, number of passivating hydrogens $N_H = 3n + 3 = 27$). For hydrogen-passivated structures, ZZH is 0.3 eV per hy-

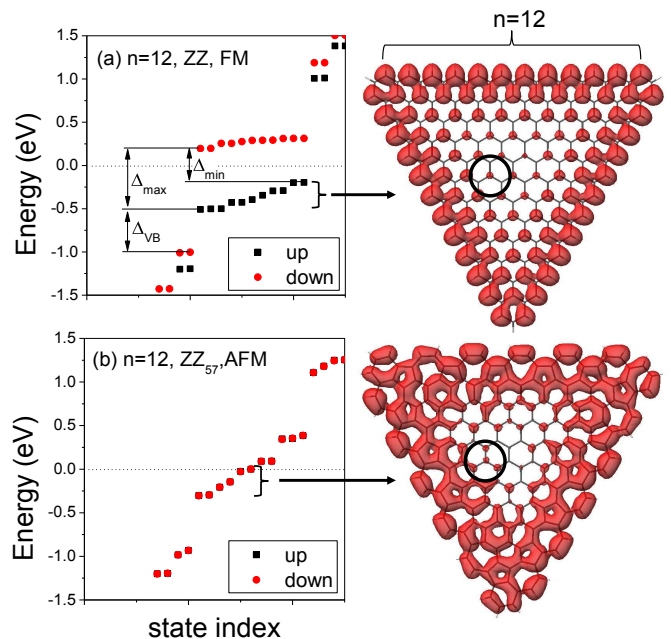


FIG. 3: (Color online) Energy spectra of the ground states for (a) ZZ and (b) ZZ_{57} configurations for a hydrogen-passivated triangular dot with $n = 12$. Spin-up states are shown in black squares and spin-down states are shown in red circles. On the right hand side, charge densities of the filled part of zero-energy bands are shown. Circular outlines show the population of only one sublattice in ZZ structure and both sublattices in ZZ_{57} .

drogen atom more stable than $ZZ_{57}H$ since in the latter structure the angles between the σ -bonds significantly deviate from the ideal 120° and the total energy is affected by strain. In the absence of hydrogen, however, the structure has to passivate the dangling σ -bonds by itself, e.g. by reconstructing the edge. Indeed, the ZZ_{57} reconstruction becomes 0.4 eV more stable. It is important to note that hydrogen passivation is a favorable process for both structures even relative to the formation of H_2 molecules and not only atomic hydrogen (Fig.2(a)). Same conclusions hold for larger TGQDs as well. These results are also consistent with the ones for graphene nanoribbons [8, 32]. Thus, we will present further only the results for hydrogen-passivated structures and will omit the index H (i.e. use ZZ instead of ZZH). In Fig.2(b), we investigate the relative stability of hydrogen-passivated ZZ and ZZ_{57} structures as a function of linear size of the triangles. The largest TGQD that we have studied has $n = 23$ atoms on a side of the triangle (622 carbon atoms total). The fact that energy per edge atom increases with size signifies that the bulk limit has not been reached yet. Clearly the ZZ structure remains the ground state for the range of sizes studied here.

It was shown previously that the number of states in the zero-energy band equals the difference between the number of atoms in A and B graphene sublattices.

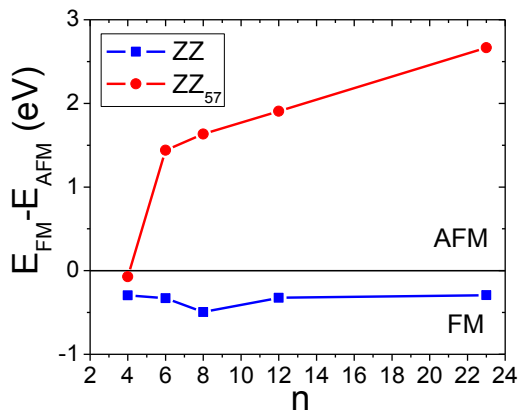


FIG. 4: (Color online) Total energy difference between ferromagnetic and antiferromagnetic states as a function of the size of the triangle for hydrogen-passivated ZZ (blue squares) and ZZ₅₇ (red circles). For ZZ the ground state is ferromagnetic for all sizes studied, while for ZZ₅₇ it is antiferromagnetic for $n > 4$

Zero-energy states are localized exclusively on the sublattice to which the ZZ edges belong and are exactly degenerate within the nearest neighbor tight-binding model[18, 19, 23]. Fig.3 compares the DFT electronic spectra near the Fermi level for the ground states of hydrogen-passivated unreconstructed (ZZ) and reconstructed (ZZ₅₇) TGQDs with $n = 12$. Introduction of the ZZ₅₇ edge reconstruction smears the distinction between sublattices. Nevertheless, the zero-energy band survives in a reconstructed (ZZ₅₇) TGQD. As can be seen from the electronic density of occupied states of the shell, they are still predominantly localized on the edges. Moreover, the number of zero-energy states remains the same. However, the dispersion of this band increases almost three-fold due to reduction of the structure symmetry. Lifting of the band degeneracy becomes observed even in the nearest neighbor tight-binding model with equal hoppings, and is more pronounced for the structures in Fig.1(c) and (d) which additionally lift the reflection symmetry present in Fig.1(b).

Magnetization of the ZZ configuration was investigated in detail through meanfield[18, 19] and exact diagonalization[21] calculations. It was shown that the electrons in the zero-energy band are spin-polarized. The up- and down-spin edge states are split around the Fermi level such that only up-spin states are filled. Our calculated dispersion of the up-spin states is ~ 0.03 eV/state (Fig.3(a)). On the other hand, the ground state of ZZ₅₇ configuration is antiferromagnetic, i.e. there is no splitting between the up- and down-spin states (Fig.3(b)). Nevertheless, calculations for the ferromagnetic ZZ₅₇ can still be performed by adjusting the Fermi level for up and down spins independently. The energy spectrum obtained in such a way is similar to the one for ZZ but with negative Δ_{min} . The interplay of the Δ_{max} and the spin-up

band dispersion in such FM calculation can be monitored to predict whether the ground state will be ferromagnetic ($\Delta_{min} > 0$) or antiferromagnetic ($\Delta_{min} < 0$). Apart from the significant increase of the band dispersion, we note that the spin up-down splitting Δ_{max} reduces by a factor of two in ZZ₅₇ structure. One can see from charge density plot in Fig.3(b) that zero-energy states can now populate both A and B sublattices even close to the center of the dot (see outlined regions). We speculate that the resulting reduction in the the peak charge density on each site is responsible for the reduced on-site repulsion between spin-up and spin-down electrons. Stronger dispersion and reduced up-down spin splitting favor kinetic energy minimization versus exchange energy and destroy the ferromagnetism in ZZ₅₇. It should be noted that partial polarization can still be possible in ZZ₅₇. Particularly, we observed it for structures with symmetric corners (Fig.1(b)) which exhibit smaller dispersion.

Our conclusions based on the analysis of the energy spectra are supported by the total energy calculations depicted in Fig.4. For ZZ structure the gap Δ_{min} is always positive and the total energy of the FM configuration is lower than that of AFM (blue squares). For ZZ₅₇ configuration, on the opposite, the ground state clearly remains AFM for all sizes with the exception of the case with $n=4$. Here the band consists of only 3 states and their dispersion cannot overcome the splitting between spin-up and spin-down states, resulting in FM configuration being more stable. The total energy difference between the FM and AFM configurations for ZZ, remains almost constant (in the range 0.3-0.5 eV) for the triangle sizes studied here, and reduces with size if divided by the number of edge atoms. Such a small value, comparable to the numerical accuracy of the method, makes it difficult to make reliable predictions regarding magnetization of larger dots.

In order to investigate whether the magnetization of the edges would be preserved on mesoscale we plot in Fig.5 the evolution of the energy spectra with the TGQD size. For this plot we performed an additional calculation for the case of $n = 40$ (1761 carbon atoms total). We did not perform the geometry optimization for this case due to high computational cost, however, based on the results for smaller structures we expect that this would have minor effect on the spectrum. This allows us to notice the reduction of the splitting Δ_{max} between the spin-up and spin-down states with the growing size, not appreciated previously[19]. Our GGA gap between zero-energy bands (Δ_{min}) and that between the valence and conduction bands are larger than LDA gaps reported previously[19], as also observed for graphene nanoribbons[41]. Both gaps show sublinear behavior, complicating the extrapolation to triangles of infinite size. This behavior, however, should change to linear for larger structures where the effect of edges reduces[22], converging both gaps to zero, as expected for Dirac fermions. An important difference

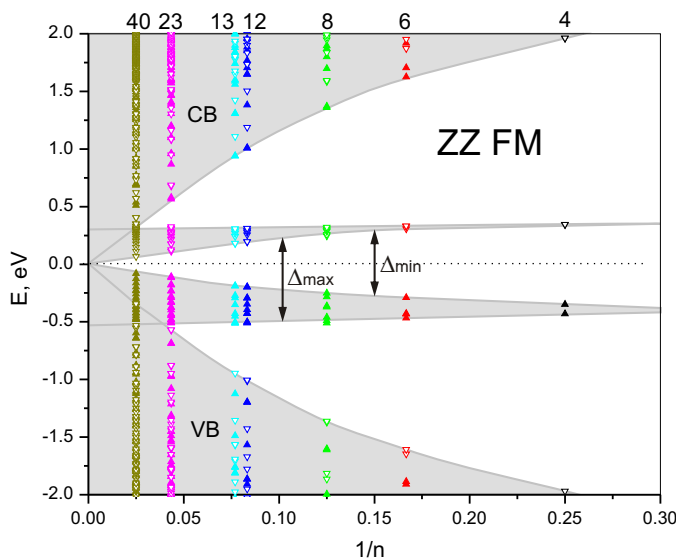


FIG. 5: (Color online) Scaling of the energy gaps with the inverse linear size of ZZ TGQDs. Full energy spectra of the structures calculated in present work are shown. Open symbols correspond to spin-down and filled ones to spin-up states.

from the nearest neighbor tight-binding calculation[23] is the growing dispersion of the zero-energy bands. Combined with the reducing valence-conduction gap, this leads to the overlap of the zero-energy band with the valence band even for finite sizes, as indeed observed for the $n = 40$ case (see Fig.5), while in ZZ₅₇ structures it becomes visible already at $n = 23$. Nevertheless, it does not affect the magnetization of the edges, as indeed confirmed by our calculation for $n = 40$, and can be compared to a magnetization of the infinitely long hydrogen-passivated nanoribbons where the edge state overlaps in energy with the valence band but in k -space those bands do not actually cross[8]. Our results thus suggest that magnetization of the edges for infinitely large triangles survives in the limit of zero temperature.

In conclusion, we have investigated the edge stability, reconstructions, hydrogen passivation in triangular graphene quantum dots and their effect on electronic and magnetic properties of the dots as a function of size. For hydrogen passivated edges, zigzag configuration is found to be more stable than pentagon-heptagon edges. The reconstruction into pentagon-heptagon zigzag edges involves a reconstruction of the triangle's corners as well, and causes the reflection symmetry to be broken. Finite magnetism is found to be destroyed in TGQDs with reconstructed (ZZ₅₇) edges, however, the band of zero-energy states survives.

Acknowledgement. The authors thank M. Korkusinski for fruitful discussions, and NRC-CNRS CRP, Canadian Institute for Advanced Research, Institute for Mi-

crostructural Sciences, and QuantumWorks for support.

- [1] K. S. Novoselov, A. K. Geim, S. V. Morozov, D. Jiang, Y. Zhang, S. V. Dubonos, I. V. Grigorieva, and A. A. Firsov, *Science* **306**, 666 (2004).
- [2] K. S. Novoselov, A. K. Geim, S. V. Morozov, D. Jiang, M. I. Katsnelson, I. V. Grigorieva, S. V. Dubonos, and A. A. Firsov, *Nature* **438**, 197 (2005).
- [3] Y. B. Zhang, Y. W. Tan, H. L. Stormer, and P. Kim, *Nature* **438**, 201 (2005).
- [4] S. Y. Zhou, G. H. Gweon, J. Graf, A. V. Fedorov, C. D. Spataru, R. D. Diehl, Y. Kopelevich, D. H. Lee, S. G. Louie, and A. Lanzara, *Nature Phys.* **2**, 595 (2006).
- [5] A. H. C. Neto, F. Guinea, N. M. R. Peres, K. S. Novoselov, and A. K. Geim, *Rev. of Mod. Phys.* **81**, 109 (2009).
- [6] K. Nakada, M. Fujita, G. Dresselhaus, and M. S. Dresselhaus, *Phys. Rev. B* **54**, 17954 (1996).
- [7] K. Wakabayashi, M. Fujita, H. Ajiki, and M. Sigrist, *Phys. Rev. B* **59**, 8271 (1999).
- [8] T. Wassmann, A. P. Seitsonen, A. M. Saitta, M. Lazzeri, and F. Mauri, *Physical Review Letters* **101**, 096402 (2008).
- [9] L. Yang, M. L. Cohen, and S. G. Louie, *Phys. Rev. Lett.* **101**, 186401 (2008).
- [10] J. Cai *et al.*, *Nano Letters* **466**, 470 (2010).
- [11] B. Wunsch, T. Stauber, and F. Guinea, *Phys. Rev. B* **77**, 035316 (2008).
- [12] J. Wurm, A. Rycerz, I. Adagideli, M. Wimmer, K. Richter, and H. U. Baranger, *Phys. Rev. Lett.* **102**, 056806 (2009).
- [13] A. R. Akhmerov and C. W. J. Beenakker, *Phys. Rev. B* **77**, 085423 (2008).
- [14] F. Libisch, C. Stampfer, and J. Burgdorfer, *Phys. Rev. B* **79**, 115423 (2009).
- [15] Z. Z. Zhang, K. Chang, and F. M. Peeters, *Phys. Rev. B* **77**, 235411 (2008).
- [16] M. Ezawa, *Phys. Rev. B* **76**, 245415 (2007).
- [17] M. Ezawa, *Phys. Rev. B* **77**, 155411 (2008).
- [18] J. Fernandez-Rossier and J. J. Palacios, *Phys. Rev. Lett.* **99**, 177204 (2007).
- [19] W. L. Wang, S. Meng, and E. Kaxiras, *Nano Letters* **8**, 241 (2008).
- [20] J. Akola, H. P. Heiskanen, and M. Manninen, *Phys. Rev. B* **77**, 193410 (2008).
- [21] A. D. Güçlü, P. Potasz, O. Voznyy, M. Korkusinski, and P. Hawrylak, *Physical Review Letters* **103**, 246805 (2009).
- [22] A. D. Güçlü, P. Potasz, and P. Hawrylak, *arxiv:1007.3527* (2010).
- [23] P. Potasz, A. D. Güçlü, and P. Hawrylak, *Physical Review B* **81**, 033403 (2010).
- [24] T. Yamamoto, T. Noguchi, and K. Watanabe, *Physical Review B* **74**, 121409 (2006).
- [25] Y. Kobayashi, K. Fukui, T. Enoki, and K. Kusakabe, *Physical Review B* **73**, 125415 (2006).
- [26] O. V. Yazyev and M. I. Katsnelson, *Physical Review Letters* **100**, 047209 (2008).
- [27] K. A. Ritter and J. W. Lyding, *Nature Materials* **8**, 235 (2009).
- [28] X. Yan, X. Cui, B. Li, Liang-Shi Li, *Nano Lett.* **10**, 1869 (2010).

- [29] J. P. Gabor, K. Zhong, M. Bosnick, M. Park, M. McEuen, *Science* **325**, 1367 (2009).
- [30] R. Baer, E. Rabani, *Nano Lett.* **10**, 3277 (2010).
- [31] A. J. Nozik, *Nano Lett.* **10**, 2735 (2010).
- [32] P. Koskinen, S. Malola, and H. Hakkinen, *Physical Review Letters* **101**, 115502 (2008).
- [33] C. O. Girit, J. C. Meyer, R. Erni, M. D. Rossell, C. Kisielowski, L. Yang, C. H. Park, M. F. Crommie, M. L. Cohen, S. G. Louie, et al., *Science* **323**, 1705 (2009).
- [34] P. Koskinen, S. Malola, and H. Hakkinen, *Physical Review B* **80**, 073401 (2009).
- [35] M. Englund, J. A. Furst, A. P. Jauho, and M. Brandbyge, *Physical Review Letters* **104**, 036807 (2010).
- [36] X. T. Jia, M. Hofmann, V. Meunier, B. G. Sumpter, J. Campos-Delgado, J. M. Romo-Herrera, H. B. Son, Y. P. Hsieh, A. Reina, J. Kong, et al., *Science* **323**, 1701 (2009).
- [37] L. C. Campos, V. R. Manfrinato, J. D. Sanchez-Yamagishi, J. Kong, and P. Jarillo-Herrero, *Nano Letters* **9**, 2600 (2009).
- [38] A. Chuvilin, J. C. Meyer, G. Algara-Siller, and U. Kaiser, *New Journal of Physics* **11**, 083019 (2009).
- [39] J. M. Soler, E. Artacho, J. D. Gale, A. Garcia, J. Junquera, P. Ordejon, and D. Sanchez-Portal, *Journal of Physics: Condensed Matter* **14**, 2745 (2002).
- [40] J. P. Perdew, K. Burke, and M. Ernzerhof, *Phys. Rev. Lett.* **77**, 3865 (1996).
- [41] E. Rudberg, P. Salek, Y. Luo, *Nano Lett.* **7**, 2211 (2007).